Easily crosslinkable side-chain azobenzene polymers for fast and persistent fixation of surface relief gratings

Guang Han [a], Hongtao Zhang [a], Jing Chen [b], Qian Sun [b], Yuying Zhang [a], Huiqi Zhang [a,*]

[a]*Key Laboratory of Functional Polymer Materials, Ministry of Education, Collaborative Innovation Center of Chemical Science and Engineering (Tianjin), and College of Chemistry, Nankai University, Tianjin 300071, P. R. China*

[b]*MOE Key Laboratory of Weak Light Nonlinear Photonics, Tianjin Key Laboratory of Photonics and Technology of Information Science, School of Physics, Nankai University, Tianjin 300071, P. R. China.*

* *Corresponding author. E-mail address:* zhanghuiqi@nankai.edu.cn (Huiqi Zhang)

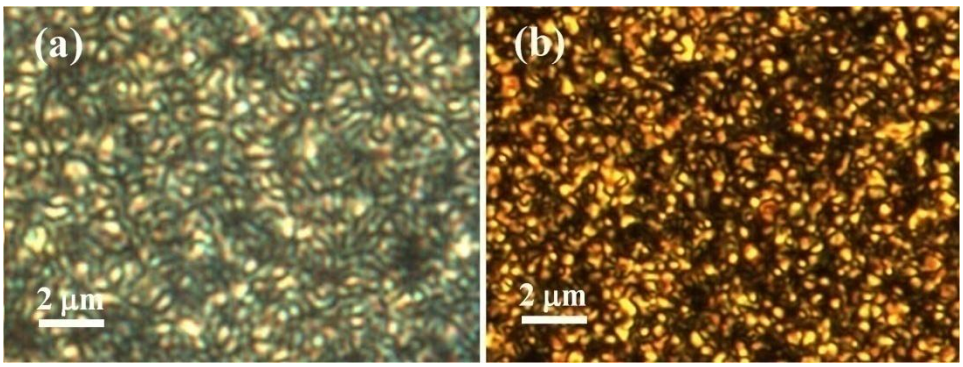

Fig. S1. POM images upon cooling form their isotropic states: (a) HP-6 at 132 ºC (annealed for 1 h); (b) HP-10 at 131 ºC (annealed for 1 h).

XRD characterization of the azo polymers

The liquid crystalline mesophases of HP-6 and HP-10 were also studied with XRD. The thin films of these azo polymers were prepared on the pre-cleaned glass plates and then annealed at their liquid crystalline temperatures for certain times (i.e., HP-6 was annealed at 132 °C for 1 h and HP-10 was annealed at 130 °C for 1 h). The resulting liquid crystalline films were then quenched with liquid nitrogen and subsequently characterized with XRD (Fig. S2a). It can be seen clearly that HP-10 exhibits one diffraction peak at the small angle area ($2\theta = 2.565^{o}$), suggesting the existence of an ordered smectic lamellar structure with a layer spacing $d = 3.44$ nm ($d = \lambda/2\sin\theta$) (Chen X, Tenneti KK, Li C, Bai Y, Wan X, Fan X, Zhou Q, Rong L, Hsiao BS. Macromolecules 2007;40:840-8). This d value is close to the calculated molecular length (l = 3.27 nm) for the fully extended liquid crystalline unit, revealing a smectic A structure, as schematically shown in Fig. S2b. On the other hand, no diffraction peak was observed for HP-6. This, together with its presence of a typical schlieren liquid crystalline texture (Fig. S1a), suggested the nematic characteristic of its liquid crystalline phase.

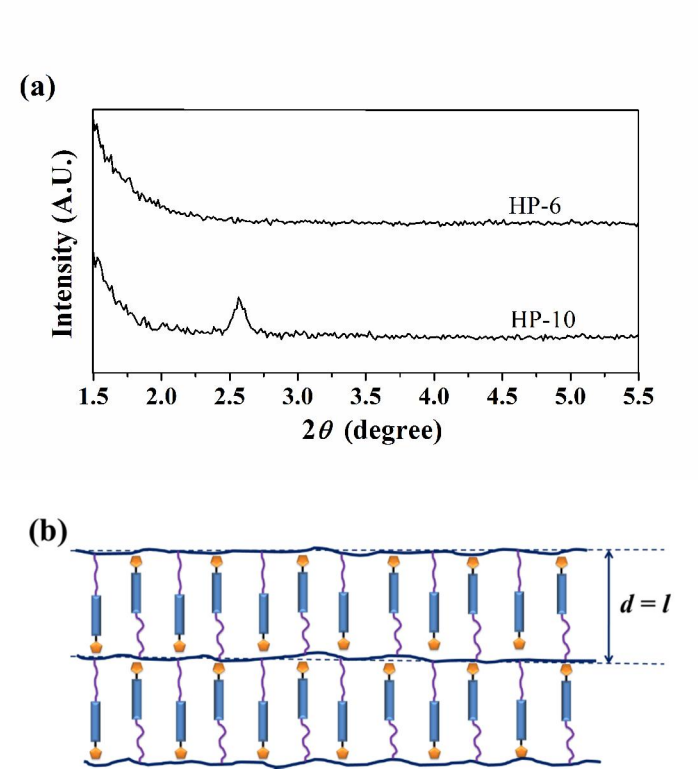

Fig. S2. XRD patterns of HP-6 and HP-10 (a) and the proposed liquid crystalline structure for HP-10 (b).

Photochemical behaviours of the azo polymer films

The photochemical behaviours of the azo polymer films were investigated by irradiating them firstly with a 365 nm UV lamp (12 W) until the photostationary state was reached and then with a 532 nm laser (10 mw/cm^2). The experimental results demonstrated clearly that the studied azo polymer films could exhibit obvious reversible photochemical isomerization upon the UV and 532 nm light irradiation (Fig. S3). Note that the finally recovered absorbance of the *trans*-azo is lower than that before UV irradiation upon the visible light irradiation (Fig. S3b,d). Similar phenomenon was also observed previously by others (Wang G, Tong X, Zhao Y. Macromolecules 2004;37:8911-7). Its real cause is not totally clear yet at this point but might be that, at the same wavelength where the *cis* to *trans* photochemical back-isomerization was performed, there was also a weak absorption from the *trans*-isomer, which eventually led to an equilibrium with *cis* to *trans* and *trans* to *cis* isomerizations taking place under the same visible light after most of the *cis*-isomer returned to the *trans*-isomer (Li

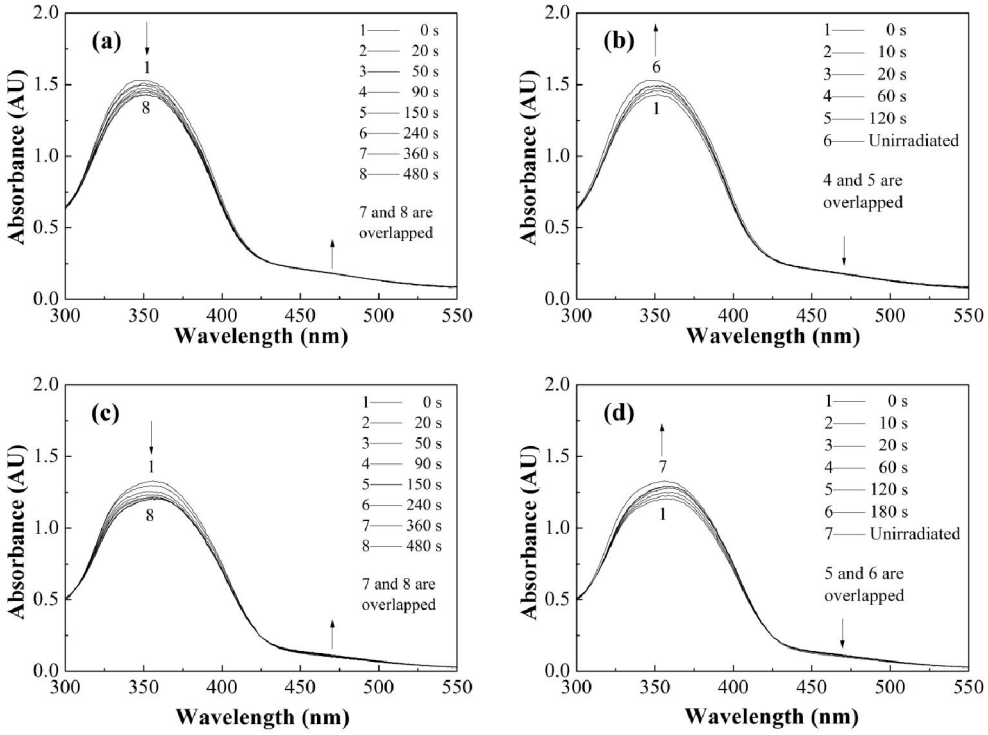

Fig. S3. UV-vis spectral changes in dependence of time for the azo polymer (HP-10 (a,b) and CP10-41% (c,d)) films at 25 ^{o}C upon irradiation with 365 nm light (a,c) and upon irradiating the film at the photostationary state with 532 nm visible light (b,d).

MH, Keller P, Li B, Wang X, Brunet M. Adv Mater 2003;15:569-72). Nevertheless, the photochemical isomerization became completely reversible upon subsequent cycles of UV and visible light irradiation (Figures not shown).

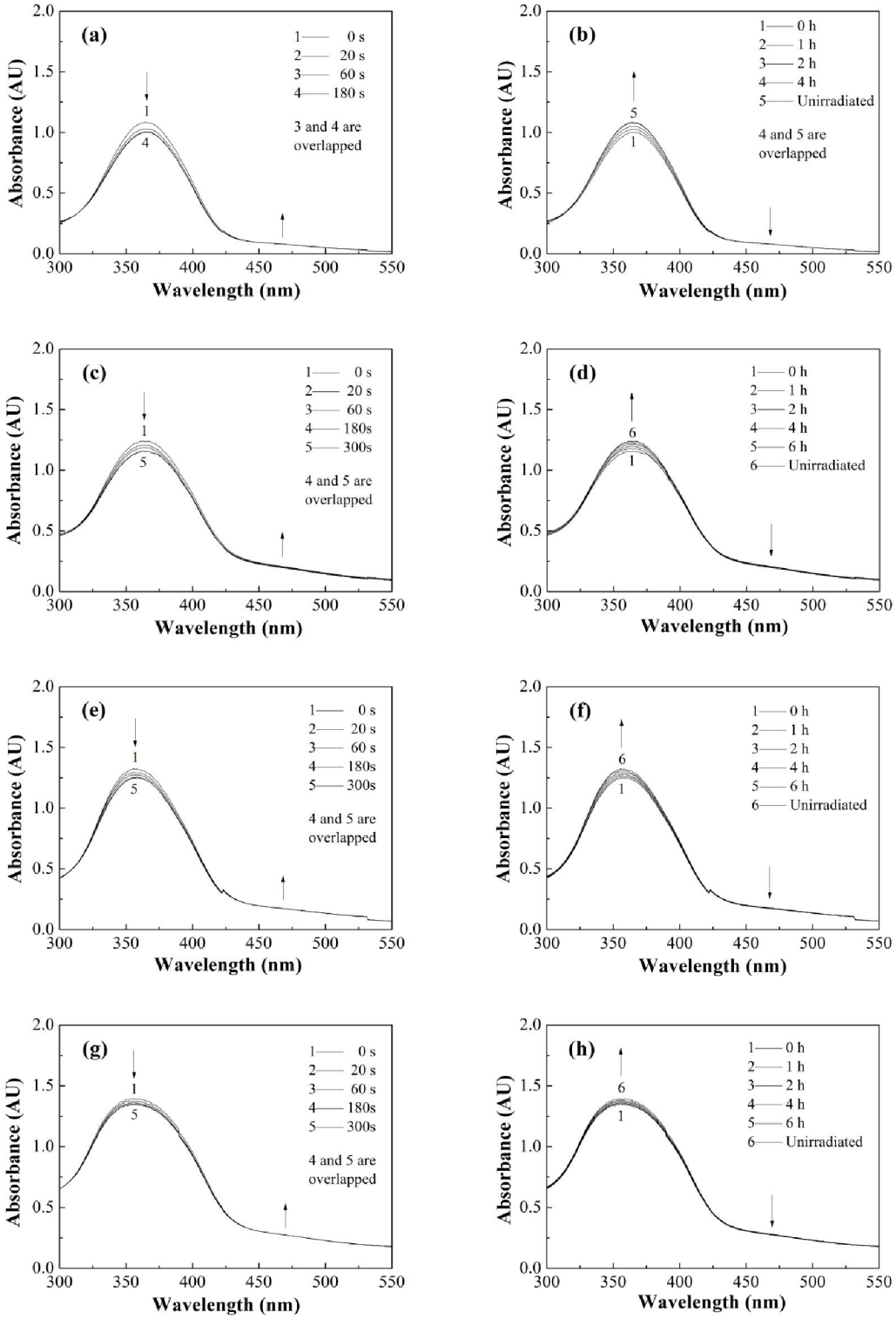

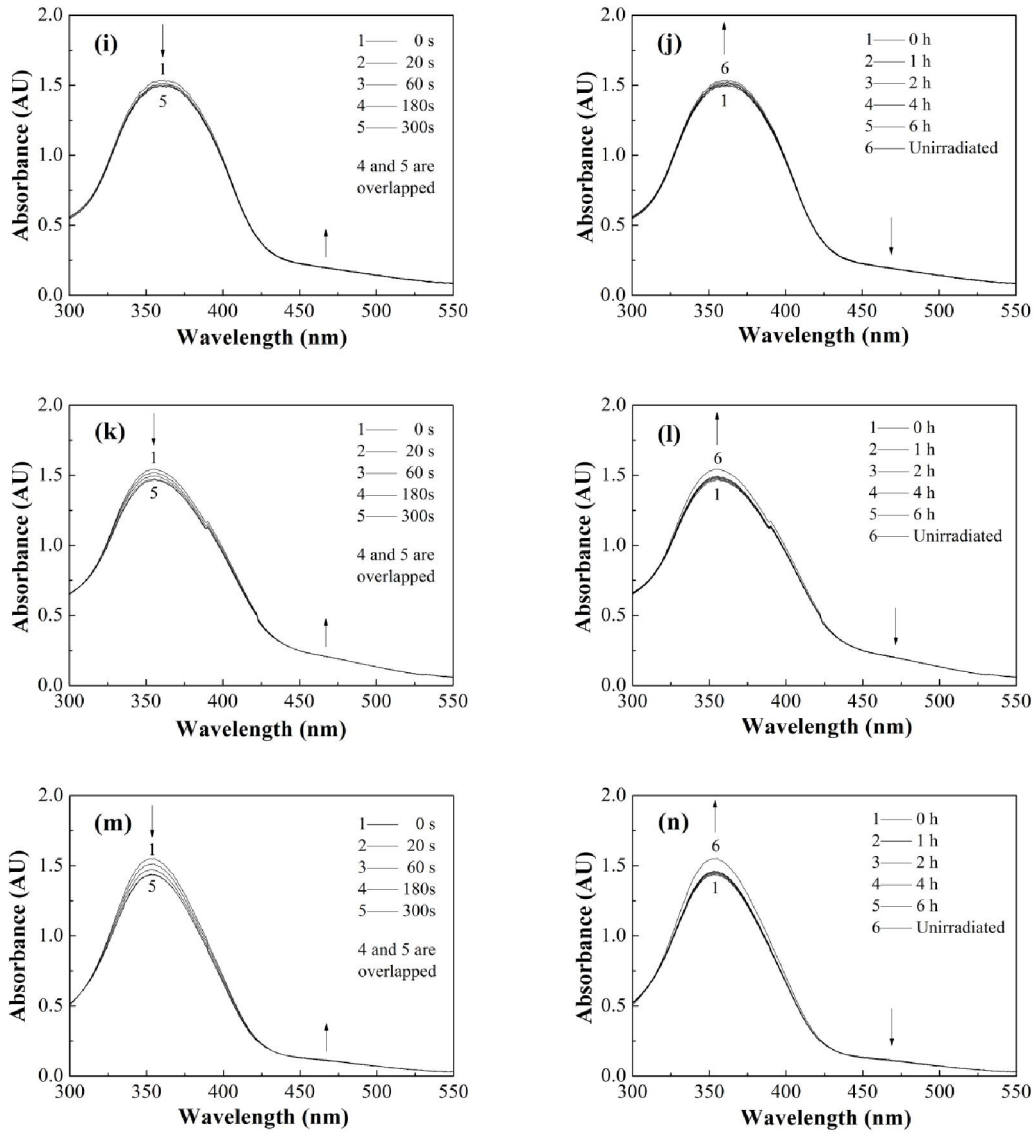

Fig. S4. UV-vis spectral changes in dependence of time for the azo polymer (CP10-15% (a,b), CP10-27% (c,d), CP10-41% (e,f), CP10-60% (g,h), HP-10 (i,j), HP-6 (k,l), HP-2 (m,n)) films at 25 ºC upon irradiation with 532 nm light (a,c,e,gi,k,m) and upon relaxing the film in the dark (b,d,f,h,j,l,n).

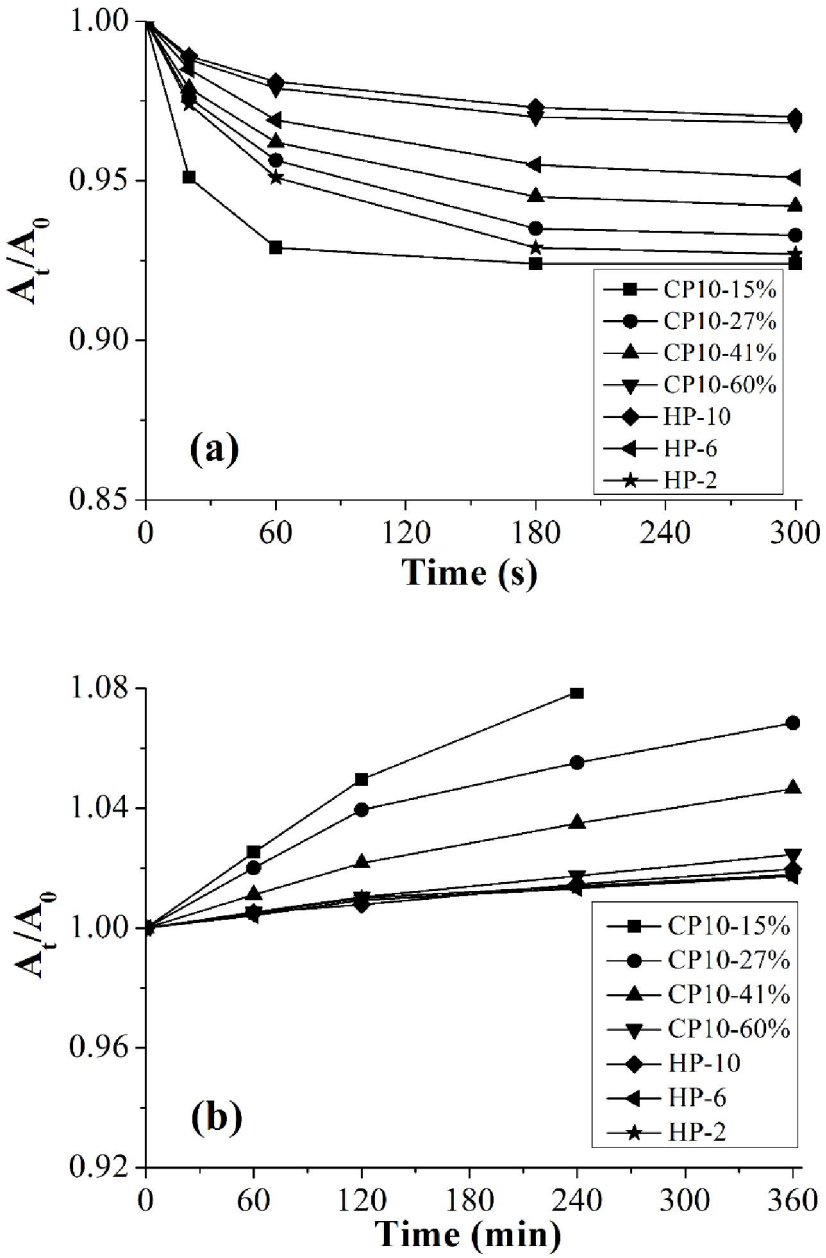

Fig. 5. (a) percentages of maximum absorption intensity of the films upon 532 nm light irradiation for different times accounting for the maximum absorption intensity of the initial film (A_t is the maximum absorption intensity of the film upon 532 nm light irradiation for t s, A_0 is the maximum absorption intensity of the initial film) (b) percentages of maximum absorption intensity of the films upon dark for different times accounting for the maximum absorption intensity of the photostationary state with 532 nm light (A_t is maximum absorption intensity of the films upon dark for t min, A_0 is the maximum absorption intensity of the photostationary state with 532 nm light) .

Table S1 The wavelength data of the maximum absorption of the polymers

Sample	Wavelength in THF (nm)[a]	Wavelength of films (nm)[b]
CP10-15%	368	365
CP10-27%	368	362
CP10-41%	368	356
CP10-60%	368	353
HP-10	368	347
HP-6	367	353
HP-2	367	356

[a] UV-vis spectra were processed by the polymers in THF solutions

[b] UV-vis spectra were processed by the polymers films

Swelling ability of the azo polymer films in methanol

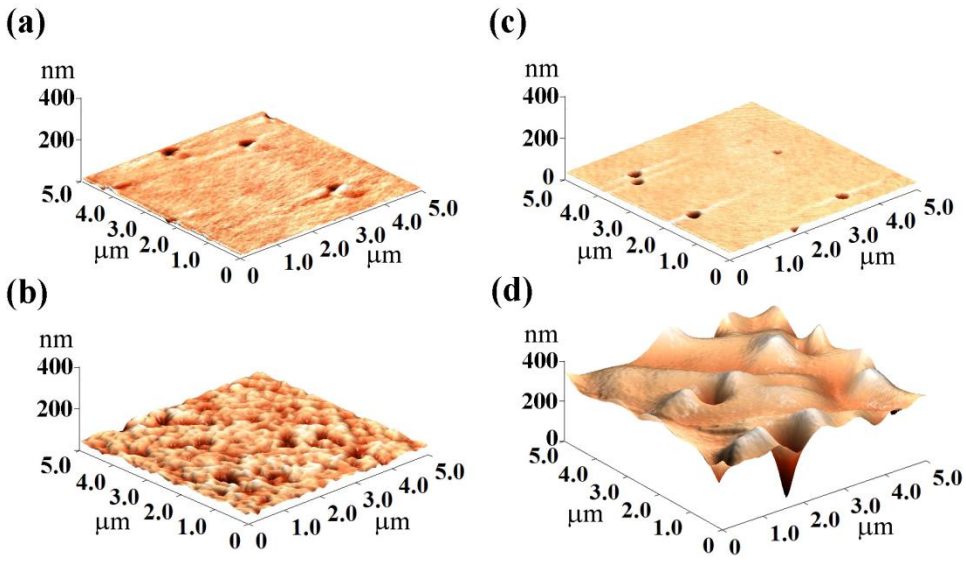

Fig. S6. Topographical AFM images of the azo homopolymer HP-10 film before (a) and after (b) its immersion into methanol for 15 min and those of the azo copolymer CP10-41% film before (c) and after (d) its immersion into methanol for 4 min, respectively.

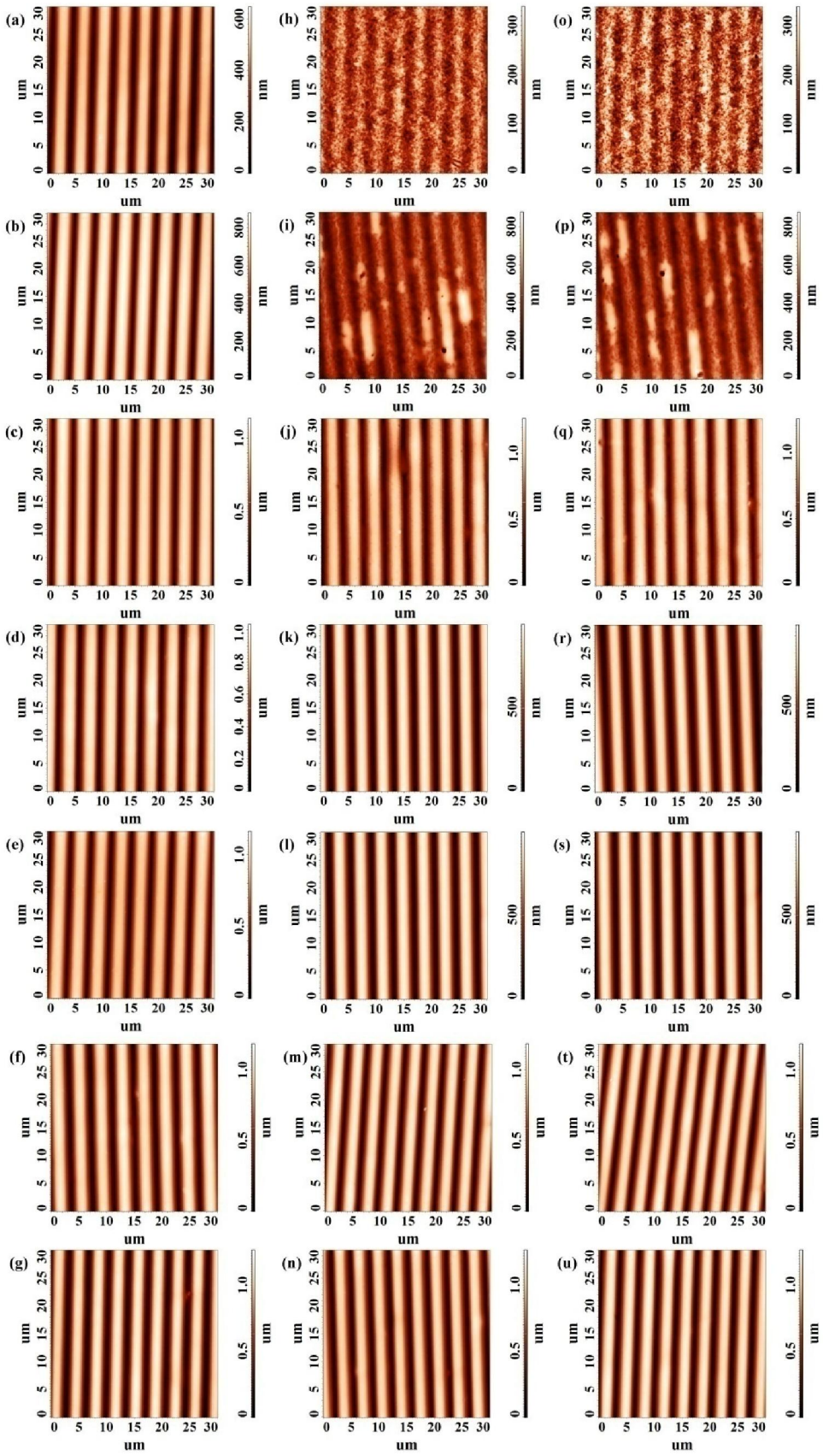

Fig. S7. AFM images of the SRGs formed on the azo polymer films under different conditions as listed in Table S2.

Table S2 The measurement conditions for AFM images of the SRGs on the azo polymer films and their modulation depth under different conditions

Sample	AFM measurement conditions [a-c]	Sequence number in Fig. S5	Modulation depth (nm) [d]
CP10-15%	Initial SRG [a]	(a)	500
	Fixed SRG for 1 min [b]	(h)	200
	Annealed SRG at 25 °C [c]	(o)	195
CP10-27%	Initial SRG [a]	(b)	780
	Fixed SRG for 2 min [b]	(i)	570
	Annealed SRG at 40 °C [c]	(p)	560
CP10-41%	Initial SRG [a]	(c)	940
	Fixed SRG for 4 min [b]	(j)	890
	Annealed SRG at 55 °C [c]	(q)	850
CP10-60%	Initial SRG [a]	(d)	945
	Fixed SRG for 12 min [b]	(k)	935
	Annealed SRG at 75 °C [c]	(r)	905
HP-10	Initial SRG [a]	(e)	960
	Fixed SRG for 15 min [b]	(l)	955
	Annealed SRG at 90 °C [c]	(s)	935
HP-6	Initial SRG [a]	(f)	1030
	Fixed SRG for 15 min [b]	(m)	1025
	Annealed SRG at 110 °C [c]	(t)	1015
HP-2	Initial SRG [a]	(g)	1170
	Fixed SRG for 15 min [b]	(n)	1160
	Annealed SRG at 140 °C [c]	(u)	1145

[a] Initial SRGs are the SRGs formed on the azo polymer films without any post-treatment.

[b] Fixed SRGs for different times refer to the SRGs post-fixed in a 1,6-hexanediamine solution in methanol with a concentration of 350 mmol/L for different times.

[c] Annealed SRGs are the post-fixed SRGs annealed at a temperature being about 10 °C above the corresponding T_g values of the uncrosslinked azo polymers for 24 h.

[d] Characterized with AFM using the tapping mode.

Effect of crosslinking on the optical transparency of the azo polymer films

The thin films of the azo polymers (HP-*m* (*m* = 2, 6, 10) and CP10-*x* (*x* = 15%, 27%, 41%, 60%)) were prepared by spin-coating following the procedure described in the Experimental section (part 2.4) in the manuscript, which were annealed at 60 °C in a vacuum oven for 12 h prior to their characterization (their thickness was about 1.1 μm as evaluated by AFM). The optical transmittivity of the above azo polymer films was determined by using an unpolarized probe He-Ne laser beam at 633 nm of a low intensity (1 mW/cm^2), which could be derived through dividing the intensity of the transmitted light by that of the incident light. Several measurements were taken across each sample, with their average being used for analysis.

The above azo polymer films were then crosslinked in a 1,6-hexanediamine solution in methanol (350 mmol/L) at ambient temperature with the crosslinking time being 1, 2, 4, 12, 15, 15, and 15 min for CP10-15%, CP10-27%, CP10-41%, CP10-60%, HP-10, HP-6, and HP-2 films, respectively. The resulting crosslinked films were washed thoroughly with methanol and then dried under vacuum at 25 °C for 12 h. The optical transmittivity of these crosslinked films was characterized following the same approach as the uncrosslinked ones.

Fig. S8 shows that the optical transparency of most of the azo polymer films was hardly affected by the crosslinking process, which is highly important for their practical applications.

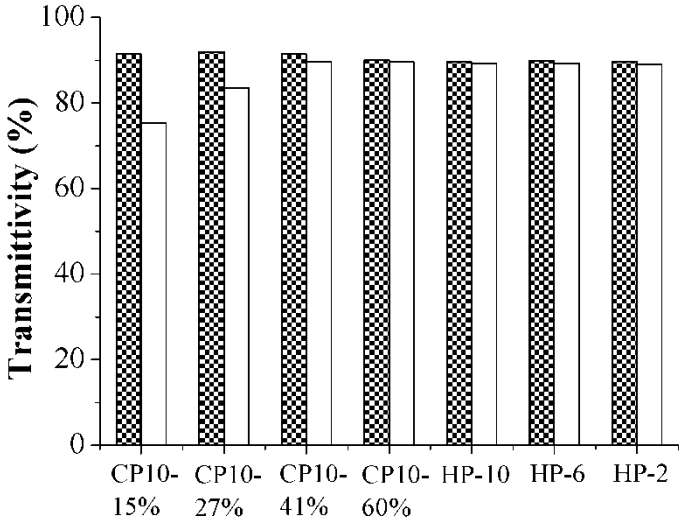

Fig. S8. The optical transmittivity of the azo polymer films before (filled columns) and after (empty columns) their crosslinking.

Effect of crosslinking on the diffraction efficiency of the azo polymer films with inscribed SRG structures

The thin films of the azo polymers HP-10 and CP10-41% were prepared following the procedure described in the Experimental section (part 2.4) in the manuscript, which were annealed at 60 ^{o}C in a vacuum oven for 12 h prior to the SRG inscription (their thickness was about 1.1 μm as evaluated by AFM). The SRG inscription was performed according to the procedure described in the Experimrntal section (part 2.5). The diffraction efficiency of these uncrosslinked azo polymer films with inscribed SRG structures was measured with an unpolarized probe He-Ne laser beam at 633 nm of a low intensity (1 mW/cm^2) in order not to disturb the SRG structures, which could be obtained through dividing the intensity of the first-order diffraction by the initial incidence intensity of the probe beam (Fig. S9). The above measurements were repeated several times across each sample, with their average being used for analysis.

The above HP-10 and CP10-41% films with inscribed SRG structures were then crosslinked in a 1,6-hexanediamine solution in methanol (350 mmol/L) with their crosslinking time being 15 and 4 min, respectively. The resulting crosslinked films were washed thoroughly with methanol and then dried under vacuum at 25 ^{o}C for 12 h. Their diffraction efficiency was measured similarly as for the uncrosslinked azo polymer films (Fig. S9).

Fig. S9 demonstrates that the diffraction efficiency of the azo polymer films was not influenced by crosslinking.

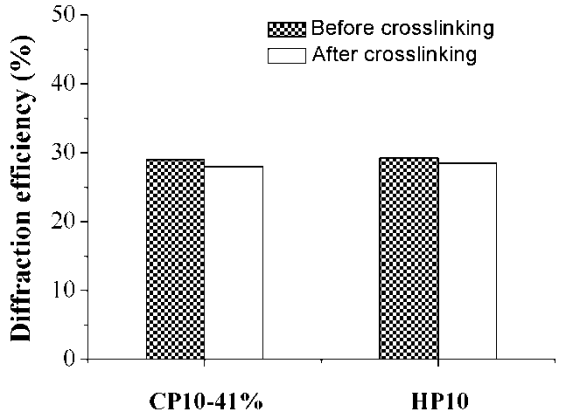

Fig. S9. The diffraction efficiency of the azo polymer films before (filled columns) and after (empty columns) crosslinking.